To appear in *Advanced Robotics*
Vol. 00, No. 00, Month 201X, 1–18

FULL PAPER

Design of 22-DOF pneumatically actuated upper body for child android 'Affetto'

Hisashi Ishihara* and Minoru Asada

Department of Adaptive Machine Systems, Graduate School of Engineering, Osaka University, 2-1 Yamadaoka, Suita City, Osaka 565-0871, Japan

(*Received 00 Month 201X; accepted 00 Month 201X*)

Child robots have been used in a lot of studies on human–robot social/physical interaction because they are suitable for safe and casual experiments. However, providing many compliant joints and lifelike exteriors to enhance their interaction potential is difficult because of the limited space available inside their bodies. In this paper, we propose an upper body structure that consists of slider crank and parallel mechanisms for linear actuators and serial mechanisms for rotary actuators. Such combinations of several joint mechanisms efficiently utilize the body space; in total, 22 degrees of freedoms (DOFs) were realized in an upper body space equivalent to that of an 80 cm tall child. A pneumatic drive system was adopted in order to fully verify the behavioral performance of the body mechanism. The proposed redundant and compact upper body mechanism can be a platform for testing the effectiveness of future exteriors for the little child android 'Affetto', which was developed in order to integrate several key characteristics for achieving advanced human–robot interaction.

Keywords: Human–robot interaction; Hybrid joint mechanism; Child android; Redundant degrees-of-freedom robot

1. Introduction

Human–robot interaction (HRI) has been receiving increased attention since robots started being considered as partners in a future symbiotic society [1, 2]. Child robots, which are designed after human children or young animals, have often been used for social/physical HRI studies [3–8]. Because they are small, light, and actuated with low-power drive system, these robots are suitable for safe and casual HRI experiments. Furthermore, interactions between caregivers and children suggest that the latter's bodies induce emotional and proactive reactions from human adults. A child robot built to have both a realistic body structure and appearance can be useful for investigating the mechanism of such interactions and thus advance HRI.

However, providing many compliant joints and lifelike exteriors to enhance their interaction potential [9] of a child-like robot is difficult because the body space is severely limited. Obviously, adding more joints to enable a wider variety of postures and motions requires more space for actuators, sensors, processors, and wiring to control them. Especially in humanoid robots, careful mechanical design is required because each body part has different roles and therefore different requirements for the joint–link structure, range of motion (ROM), and joint torques. For example, the shoulder mechanism should enable wide and complex arm movements, while the lumbar mechanism must support the heavy weight of all of the other upper body parts. Thus, the lumbar mechanism can take up a larger cylindrical space in the abdominal part despite its motion being simpler than that of the shoulder mechanism.

*Corresponding author. Email: ishihara@ams.eng.osaka-u.ac.jp

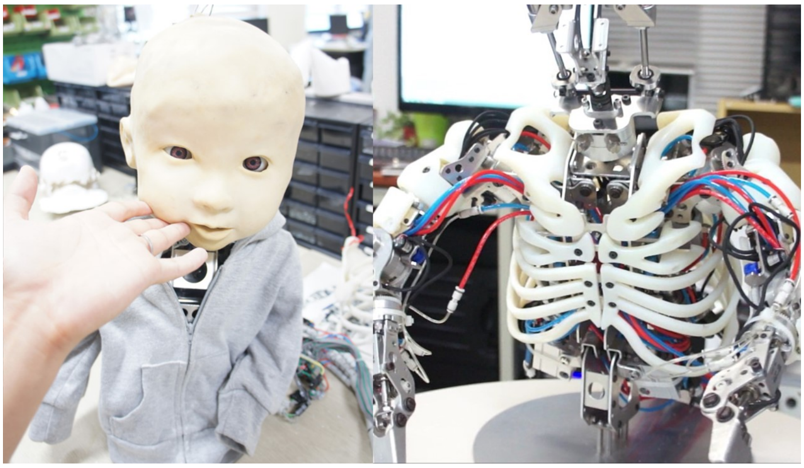

Figure 1. Appearances of child android 'Affetto' with its head and clothes on (left) and off (right).

When robots are expected to have lifelike exteriors, the design issues are more severe. Some child robots have thick soft coverings for more safety and comfort [10, 11], while others have a smooth surface with a lifelike appearance to provide the visual illusion that they are real [12, 13]. Some systems install tactile sensors in the exterior to enrich communications with humans [14]. The problem is that such lifelike and soft exteriors need farther dedicated space in the body because they require an additional shell-like tough exterior inside to support them.

Thus, designing a child robot with many joints and lifelike exteriors is technically challenging but may help in advancing HRI studies. To overcome this design issue, the limited space available inside the body must be allocated to appropriate functions effectively and efficiently. Appropriate types of actuators and joint mechanisms should be utilized for different body parts because their required specifications are completely different.

In this paper, we propose an humanoid-type upper body robot consisting of slider crank and parallel mechanisms for linear actuators and serial mechanisms for rotary actuators. Such combinations of several joint mechanisms efficiently utilize a body space; in total, 22 degrees of freedom (DOFs) were realized in an upper body space equivalent to that of an 80 cm tall child. A pneumatic drive system was adopted in order to fully verify the behavioral performance of the body mechanism and realize whole-body passive coordinated movement against external forces; the drive system enables both high-speed compliant joint actuation and long hours of operation without overheating. The proposed upper body can be a platform for testing the effectiveness of future exteriors for the child android 'Affetto' [15] (see Fig. 1). This was developed with the aim of integrating several key characteristics for achieving advanced HRI. These characteristics and future issues were evaluated based on a survey of existing child robots.

2. System requirements

2.1 *Size, shape, and weight*

The size, shape, and weight of a robot are the most important design elements because they influence the first impression of the robot and are dominant kinematic and dynamic parameters. We determined the size of each body part of our robot by referring to the measured data of male Japanese children [16]. We targeted the size data of children 12–23 month old. Because children's motor and social skills are known to develop dramatically during these ages, at this size we can use our robot with various sophisticated control algorithms without giving a sense of incompatibility to participants in HRI experiments. The determined height and weight for the entire body (with head, hand, and legs) were 80 cm and 12.4 kg, respectively. The sizes of all body parts were determined based on the actual measured child data, which included the length

Table 1. Specifications of each joint: name of motion, estimated required torque, adopted mechanism type, theoretical peak torque, and realized range of motion.

Joint number	Motion	Required torque [Nm]	Mechanism type	Realized torque [Nm]	Range of motion[deg]
J1	Neck flexion (extension)	2.4	PM	9.1	60
J2	Neck lateral flexion	2.4	PM	14.1	67
J3	Neck lateral rotation	0.12	DD	2.0	100
J4(11)	Shoulder elevation	2.1	SC	5.5	22
J5(12)	Shoulder abduction	1.3	SC	4.5	61
J6(13)	Shoulder flexion	1.3	DD	2.0	100
J7(14)	Shoulder rotation	0.04	DD	0.9	100
J8(15)	Elbow flexion	0.32	DD	0.9	100
J9(16)	Forearm pronation	0.001	DD	0.2	180
J10(17)	Wrist flexion	0.03	SC	0.8	28
J18	Chest rotation	1.73	DD	2.0	28
J19, J21	Waist lateral bending	5.1	PM	18.8, 14.6	40, 30
J20, J22	Waist flexion (extension)	6.7	PM	13.2, 17.6	38, 32

DD=Direct Drive, SC=Slider Crank, PM=Parallel Mechanism

of the upper arms (15.3 cm), thickness of the chest (12.6 cm), and shoulder width (19.9 cm).

2.2 *Number of joints*

Although determining how many joints are sufficient for HRI is difficult, the location and number of redundant joints should be similar to those of humans; this not only widens the variety of behavioral expressions but also may help induce intuitive interactions with robots. Joints in the shoulder, chest, and waist have often been excluded from robot bodies because they are kinematically redundant, make precise posture control difficult, cost weight and space, and are totally expensive. However, they can be useful for HRI because kinematic redundancy lets robots adapt to an dynamic environment, and these joints contributes to several expressive gestures such as breathing motions, shoulder shrugs, and chest shaking from excitement. Therefore, we adopted redundant joints. Table 1 summarizes the adopted joint motions.

2.3 *Joint torques*

The required joint torques were estimated with a simplified dynamics model that comprises several cylindrical body parts whose sizes were determined based on the child data [16]. To estimate the required torque for each joint, the maximum anti-gravity torque and acceleration torque for an angular acceleration of 4π rad/s^2 to rotate each joint $\pi/2$ rad in 0.5 s were calculated. Table 1 summarizes the estimated torques required for all joints.

2.4 *Control system and power supply*

A difficult decision was where the power supply system and precision control devices should be placed. Considering the tradeoff between the mobility and variety of upper torso movements, we decided to place them outside the robot because the inclusion of such a system and devices inside the robot seriously reduce the space for joints and mechanisms while increasing the robot weight which severely affect the interaction performance of the robot.

2.5 *Robustness against external forces*

When robots are used in physical HRI experiments, unexpected external forces capable of breaking these robots may be applied. To prevent such an undesirable situation, experimenters have restricted close physical interaction between participants and robots or adopted robots with fewer joints or a thick soft covering. In order to increase the close interactions between humans and robots, we adopted a shock-resistant drive system and a redundant number of compliant joints to endure and distribute external forces.

2.6 *Safety mechanism*

Another reason why experimenters have restricted close physical interaction is unexpected intense contact can be dangerous for humans. A slim and lightweight joint drive system with passive compliance is desirable for this aim because it can contribute to safety. Moreover, it allows more space to be utilized for an additional shock-absorbing soft exterior. Therefore, we designed the joint system with passive compliance to be as slim and light as possible.

We also adopted instant and reliable deactivation of the drive system. Especially when we utilize the designed upper body for physical/social HRI experiments, every joint should lose its power and become a free joint instantly for safety.

3. Design

Figure 2 shows a computer-aided design (CAD) image of the upper body. Its joint mechanism comprises several sub-mechanisms: a neck mechanism, a pair of shoulder mechanisms, a pair of arm mechanisms, and a lumbar mechanism. In this paper, we use the letters R, B, P, U, and S to denote roll, bend, prismatic, universal, and spherical joints, respectively, for their kinematic chains. Underlined letters denote the joints actuated in parallel mechanisms while italic letters denote the joints realized with slider crank mechanisms. In total, this body has 22 DOFs. The neck has three DOFs (1R and 2S$\underline{\mathrm{P}}$U-U parallel mechanism), the shoulder has three DOFs (R*BB*), the arm has five DOFs (RRBR*B*), and the lumbar region has four DOFs (serially coupled 2S$\underline{\mathrm{P}}$U-U). The details of these mechanisms are explained in section 3.1.2. For all of these DOFs, we selected air cylinders or air vane rotary actuators (hereafter, air rotors).

Bone-shaped semi-hard exteriors were attached to the joint mechanisms. These exteriors were made of flexible plastic intermingled with a rubber-like material produced by a 3D printer (Objet260 Connex$^{\mathrm{TM}}$). The bone shape provides a realistic structure for a skin layer structure to be attached to in the future, and its flexibility helps absorb shocks such as those caused by interaction with humans to protect the joint mechanisms.

Figure 3 shows an overview of our robot system. This is a standard setup to achieve position/stiffness control of air cylinders and rotors [17, 18]. This system can be divided into three subsystems: a body system, power supply system, and control system. The body system includes actuators, joint mechanisms, and two kinds of internal sensors: potentiometers and pressure transmitters. The control system is connected to the other systems with electric cables to monitor the sensors and operate the power supply system. The details of these subsystems are given in the following subsections.

3.1 *Body system*

3.1.1 Actuators and sensors

Air cylinders and rotors were considered to be appropriate for our robot for several reasons:

(1) The high compressibility of air provides the joints with passive compliance. In addition,

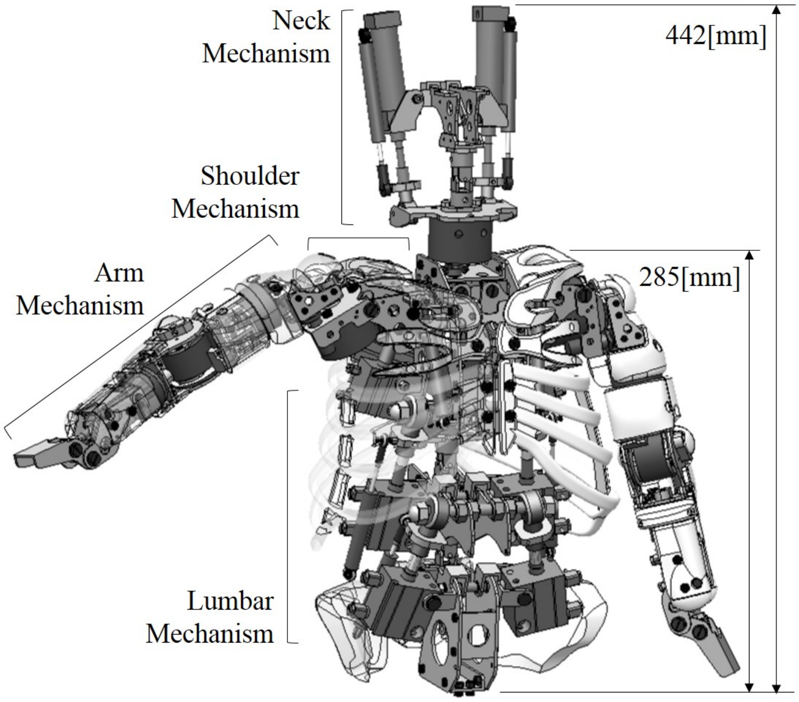

Figure 2. CAD image of upper body: divisions of mechanisms and approximate sizes.

Table 2. General properties of several joint mechanisms for air cylinders and air rotors.

Mechanism type	Shape	Volume density	Torque	ROM
Direct Drive (air rotor)	Cylindrical	High	Small	Large
Slider Crank (air cylinder)	Wide and thin rectangle	Middle	Middle	Middle
Parallel Mechanism (air cylinders)	Cylindrical	Low	Large	Middle

their spring and damper characteristics can be controlled with appropriate controllers.

(2) They can generate a large amount of power in two directions without reduction gears, which reduce the actuation speed and backdrivability.

(3) They can be deactivated securely and instantly by exhausting air even when their electric control devices do not work properly.

(4) They are difficult to break because their structures are mechanically simple and their components such as drive shafts and casings has high rigidity.

Each air cylinder (SMC CUJ) and rotor (SMC CRB2) has two air chambers, whose inside pressures p^+ and p^- drive the actuator shaft. The ideal output force without both frictions and any other external forces is proportional to the subtraction of these pressures. To monitor the shaft positions and inside pressures, potentiometers (Copal Electronics JC1003 and JC10) and air pressure transmitters (SMC PSE530) were installed.

3.1.2 Joint mechanism

We determined an appropriate joint mechanism for each joint by considering the mechanical properties of each mechanism. Table 2 summarizes the candidate mechanisms and their properties.

First, a direct drive mechanism with an air rotor is effective for constructing compact cylindrical bodies with several joints because complex mechanical parts such as long linkages are not

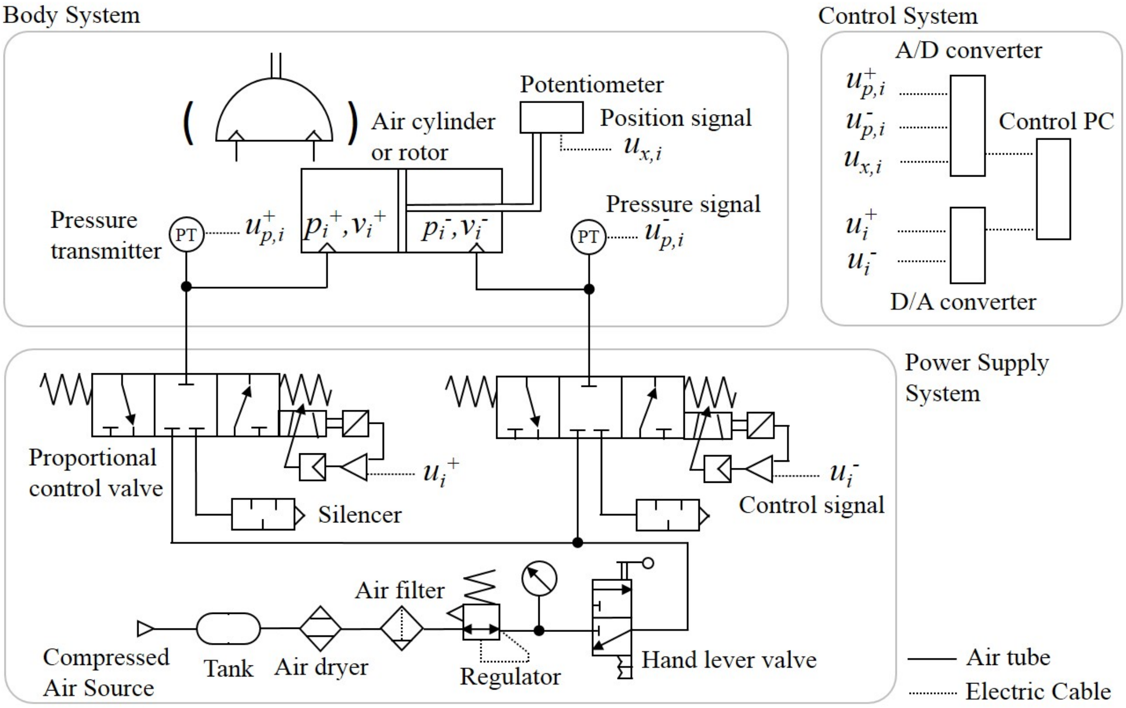

Figure 3. System overview.

necessary. A broad ROM over 90 deg can be achieved by this mechanism, while output torques are small without reduction gears. Therefore, we adopted this mechanism for the arms, which have cylindrical bodies and require large ROMs.

Second, a slider crank mechanism with an air cylinder is appropriate for single-DOF joints requiring large torques if wide spaces for long linkages are available. Although this mechanism can essentially realize infinite rotation, its ROM should be limited to an adequate range for which several singular points do not exist for stable motion control. We adopted this mechanism for the shoulder, which requires larger torques than the arm and has a thin and wide space.

Third, a parallel mechanism with several air cylinders is effective for multi-DOF joints requiring large torques because several actuators can share loads against these joints. Instead, this mechanism occupies a large amount of space owing to wide range movements of several linkages. We adopted this mechanism for the neck and lumbar region because they need to support heavy body parts but have large spaces in the head and abdomen. There is a considerable volume of openings in this mechanism and therefore careful mechanical design enables other joint mechanisms to utilize these openings.

Table 1 summarizes the determined mechanism type, its theoretical peak torque with 0.7 MPa air pressure, and its ROM for each joint. Figures 4, 5, 6, and 7 show the joint mechanism details for each body part of our robot. The three-dimensional neck is realized with a two-dimensional 2S$\underline{\text{P}}$U-U parallel mechanism for both neck flexion (J1) and neck lateral flexion (J2) and a 1R joint for neck lateral rotation (J3). The three-dimensional shoulder is an RBB mechanism, whose bend joints for shoulder elevation (J4) and abduction (J5) are serially-coupled swinging block slider crank mechanisms. These slider crank mechanisms are installed to shift in front and behind each other so that they can share the space as efficiently as possible. The arm is a five-dimensional RRBRB serial mechanism, that is basically realized with direct drive mechanisms. The lumbar region uses four-dimensional serially coupled 2S$\underline{\text{P}}$U-U parallel mechanisms to achieve both large ROMs and sufficient torques. Air cylinders for waist lateral bending (J19 and J20) and waist flexion (J20 and J22) are attached to be tilted forward so that they can utilize their opposing number's openings efficiently.

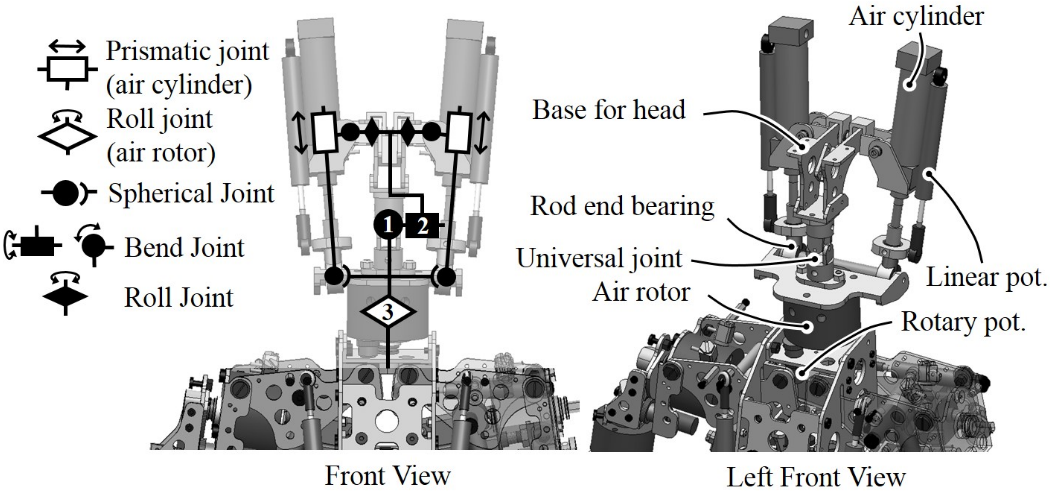

Figure 4. Two-dimensional 2S$\underline{\text{P}}$U-U parallel mechanism and 1R joint for neck.

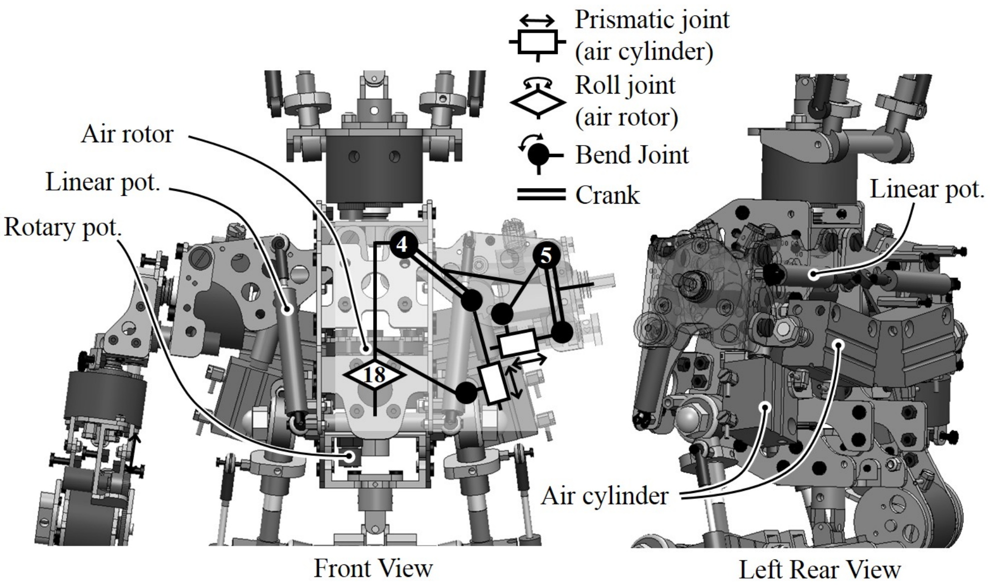

Figure 5. RBB shoulder mechanism, whose bend joints (J4 and J5) are serially coupled swinging block slider crank mechanisms. These slider crank mechanisms are described side by side in the front view but are actually installed to shift in front and behind each other.

3.2 *Power supply and control systems*

The power supply system provides clean and regular pressurized air to proportional flow control valves (Festo MPYE-5-M5-010-B), each of which is connected to one chamber of the actuator. The valve can control both the air intake flow rate to the chamber and the exhaust flow rate from the chamber to the atmosphere according to a control voltage. When the control voltage is 0–5 V, the valve enables the intake of the regular pressurized air, whose flow rate is inversely proportional to the voltage. On the other hand, the air in the chamber can be exhausted when the voltage is 5–10 V, and the exhaust flow rate is directly proportional to the voltage. The inside pressures p^+ and p^- in two chambers of an actuator can be controlled by precise adjustment of a pair of control voltages $\boldsymbol{u}^+$ and $\boldsymbol{u}^-$. Theoretically, a pair of the valves are favorable to realize position, speed, and stiffness control of air cylinders or rotors [17–21].

The tube length between the chamber and valve should be as short as possible to minimize the

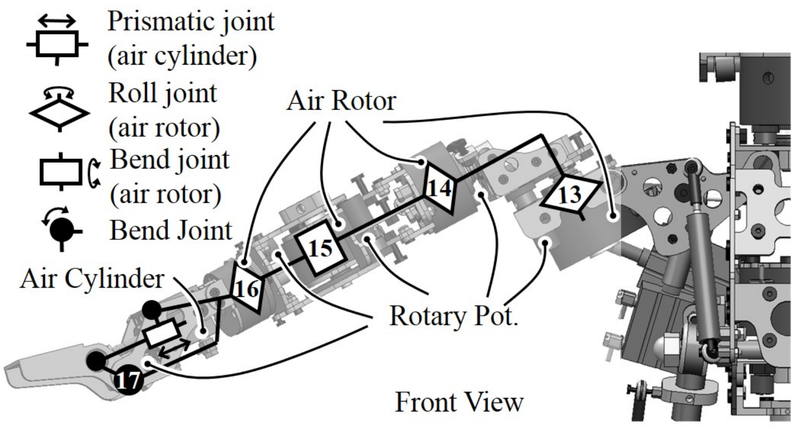

Figure 6. RRBRB serial arm mechanism, whose one bend joint is realized with a swinging block slider crank mechanism.

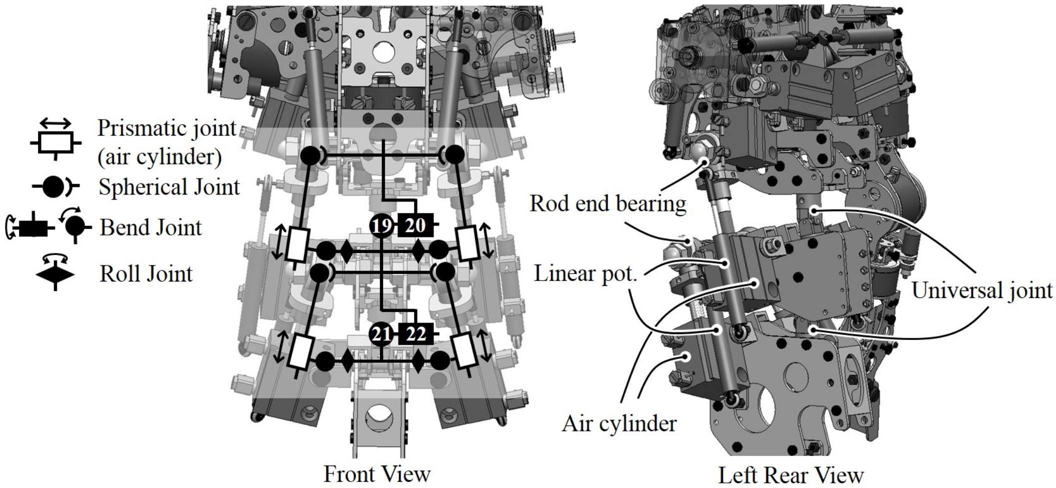

Figure 7. Four-dimensional lumbar mechanism realized with serially-coupled 2S$\underline{\text{P}}$U-U parallel mechanisms.

pressure transfer delay and pressure loss. Nonetheless, a certain length is necessary to install the valves at a distant place that does not obstruct the body movement. We adopted polyurethane air tubes with a 2 mm internal diameter to minimize the pressure delay and loss for air 1.5 m long tubes.

A personal computer with D/A converter boards (Contec AIO-163202F and AD12-16) and A/D boards (Contec DA12-16) was used ot receive signal voltages from the internal sensors and determine the control voltages for the valves at a frequency of 100 Hz.

4. Dynamic performance

Dynamic performance of the robot was evaluated in agility, accuracy, and passive compliance. A movie of its movement can be found at an online repository [22].

4.1 *Agility*

We tested whether our system can provide the expected dynamic performance. Figure 8(a) and (b) show how the actuators reacted when we instantly changed the control voltages by large amount. First, we set the voltage of one valve $\boldsymbol{u}^{+}$ to 8 V and the other valve $\boldsymbol{u}^{-}$ to 2 V for

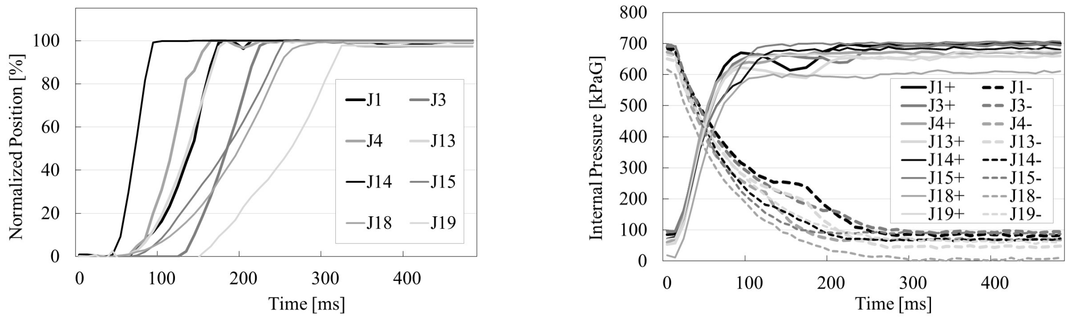

(a) (b)

Figure 8. Reaction of actuators to large instantaneous change in their control voltages. The regular pressure provided to all valves was 0.7 MPaG in this experiment. The shaft positions of the actuators were normalized by their maximum ranges, and their positive directions for their joints were opposite the direction of gravity. (a) Normalized positions of shaft of air actuators (b) Internal pressures p^+ and p^- of air actuators

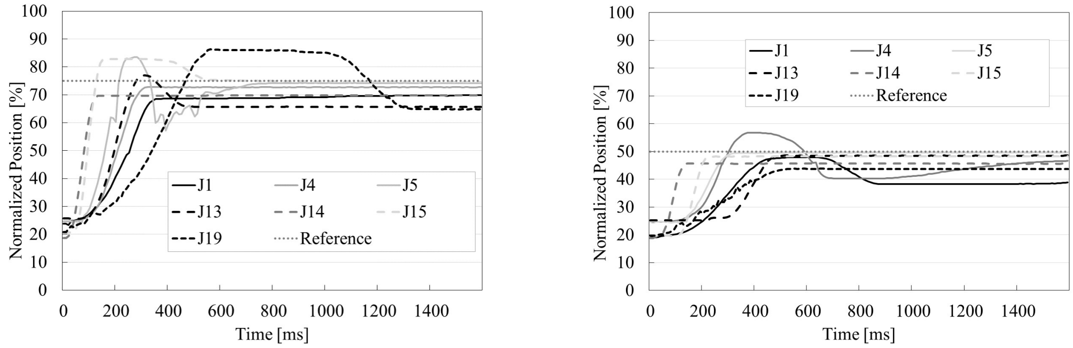

(a) (b)

Figure 9. Normalized position trajectories for typical 8 of 22 DOFs when reference position changed at time 0 ms. (a) Reference changes from 25% to 75% (b) Reference changes from 25% to 50%

each actuator. Then we switched these voltages at the time of 0 ms to drive the actuators' shaft from one end of their ROM to the other end. This operation was executed for every actuator, one after the other in upright posture. After the voltages were switched, the internal pressure in one chamber for each actuator gradually increased, and the pressure in another chamber decreased, as shown in Fig. 8(b). When the time was around 50 ms, the magnitude relation of these pressures was reversed. This was the maximum pressure transfer time of our system. Several actuators did not start to move even after the time because of the large static friction of their shaft and large loads against them. Despite this delay, every actuator reached their other end with 320 ms at the latest. This result shows that the required torques are sufficient to realize the required joint speed described in 2.3.

4.2 *Accuracy*

We applied a proportional-integral-derivative (PID) controller with pressure feedback and simple friction compensation to these actuators. The pairs of valve control voltages $\boldsymbol{u}^+(t)$ and $\boldsymbol{u}^-(t)$ at the discrete time t for each actuator were calculated as

$$\boldsymbol{u}^{+}(t) = 5 + k_P\boldsymbol{e}(t) + k_D\dot{\boldsymbol{e}}(t) + k_I\int_0^t \boldsymbol{e}(s)ds - k_F(p^{+}(t) - p^{-}(t)) + f, \tag{1a}$$

$$\boldsymbol{u}^{-}(t) = 5 - k_P\boldsymbol{e}(t) - k_D\dot{\boldsymbol{e}}(t) - k_I\int_0^t \boldsymbol{e}(s)ds + k_F(p^{+}(t) - p^{-}(t)) - f, \tag{1b}$$

where $\boldsymbol{e}(t)$ denotes the error deviation calculated as $\boldsymbol{x}' - \boldsymbol{x}(t)$, $\boldsymbol{x}'$ denotes the reference position of an actuator shaft, $\boldsymbol{x}$ denotes the current position of the shaft, and f denotes the friction compensation constant. Actual calculation is based on discretized forms of equations (1a) and (1b). Figure 9(a) and (b) show typical normalized position trajectories for several actuators when their target positions were first set to 25% of their range and then changed to 75% or 50% at time of 0 ms. This operation was also conducted for every actuator one by one. Positions converged to within 10% around the reference after about 600 ms in most cases. Although control accuracy to this degree is not sufficient for object manipulation or balance control, several gesture postures or movements can be achieved with this controller. To achieve more accurate position control in the future, we can utilize several position controllers [18–20] to compensate for both the hysteretic characteristics of the shaft friction force [23, 24] and compressibility of supplied air (see the survey [21]).

4.3 *Passive compliance*

Finally, we evaluated the joint compliance of our robot with the above controller. The reference positions for every joint were set to 50% of their range and a high-frequency external force was applied to the wrists of the robot. After joint positions are well converged, we grabbed the wrists and manually shook them in various directions as fast as possible. Although actual applied force was not measured in this experiment, we applied as much force as typically required for shaking children's relaxed arms. Figure 10 shows typical normalized position trajectories for several joints in the arm and shoulder. We grabbed the wrists at time of 500 ms and started to shake at time of 2000 ms. This figure shows that the joints followed a high-frequency shaking motion around 4 Hz with no compliance controller due to the high compressibility of air. Although each joint's compliance depends on its internal pressures and should be measured quantitatively for future work, this result indicates the desirable degree of passive compliance for physical HRI.

5. Discussion

The characteristics of the proposed upper body can be summarized as follows:

(1) mechanical softness (pneumatic drive system and semi-hard exteriors)
(2) agility (full range motions in 320 ms without control or 600 ms with position controllers)
(3) lifelike surface (realistic shape of each body part of a child, including bones)
(4) humanlike redundant DOFs (22 DOFs), and
(5) childlike figure (realistic size of each body part of a child).

These characteristics seem essential for HRI to be effective; therefore, some have been adopted into several child robots. In the following, we discuss how each characteristic has been realized in child robots and how they affect HRI.

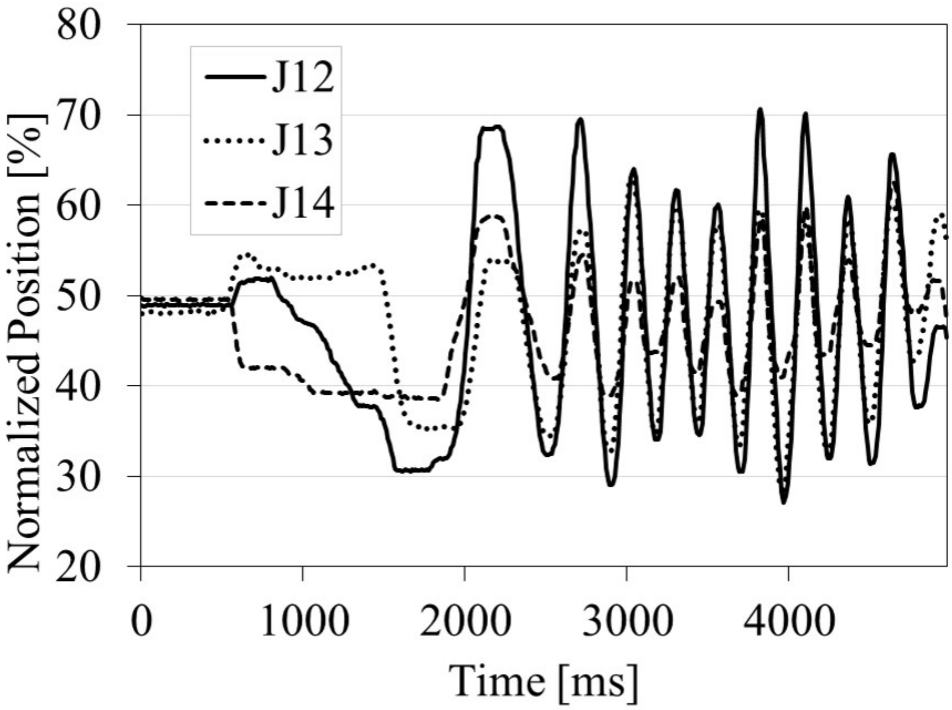

Figure 10. Normalized position trajectories for typical three DOFs when high-frequency external force was applied to wrists. We grabbed the wrists at time of 500 ms and started to shake them manually at time of 2000 ms.

5.1 *Mechanical softness*

Several child robots have adopted compliant joints and elastic exteriors. Compliant joints are often achieved by actuators with mechanical softness such as pneumatic ones. For example, Pneuborn-7II, -7III, and -13 [25] have antagonistically attached Mckibben pneumatic artificial muscles, which have a rubber balloon as the main component. Such pneumatic actuators are suitable for constructing a complex musculoskeletal system with large DOFs and bi-articular muscles because of the high power–weight ratio and structural flexibility. On the other hand, their rich flexibility makes model-based control much more difficult. Air cylinders or rotors are easier to control than Mckibben muscles because they have rigid casing and have been utilized in CB^2 [14] and Diego-san [26]. In general, pneumatic drive systems allow high-speed actuation with high torque and high backdrivability to joints.

Other child robots have realized joint compliance by utilizing a hybrid actuation system of electric geared motors with flexible materials such as rubber bands [27, 28]. Although this combination allows for more precise model-based control, it is difficult to achieve both high-speed and high-torque actuation.

Soft materials are often attached onto robot surfaces for safe contact and/or comfortable tactile sensation to humans especially when they are expected to be intensively touched by humans. While most child robots have partial soft coverings [29–31] or no ones [32, 33], some have whole-body coverings made with soft materials such as soft vinyl, elastomatic form, or cotton cushion [4, 10, 11, 34, 35]. Although their compressibility and flexibility are effective at absorbing shock, it is not easy to realize high-motion performance because they are not easy to stretch and thus interfere with the joint motions. CB^2 [14] and Repliee-R1 [12] have silicone rubber, which has high elasticity, as their coverings to achieve a skin-like texture. However, this is heavier and absorbs less shock than form or cushion materials.

Thus, there are several methods to achieve mechanical softness in joints and exteriors for child robots. However, these seems to be a tradeoff between the mechanical softness and motion performance. Therefore, designers should carefully decide which method should be chosen for their robots.

5.2 *Agility*

The ability to move quickly could be sometimes needed for natural HRI. In human–human interaction, our behavior rhythms tend to synchronize with each other, and such synchronization can facilitate the smoothness of interactions and increase mutual preference [36, 37].

Such synchronization can also be seen in HRI and can improve positive impressions of the robot[38]. Excited rhythmic motions are considered to trigger synchronized interaction, and Keepon [4] was designed based on this idea. To achieve sufficiently high agility for excited rhythmic motions, its small snowman-like body is hollow. Moreover, actuators and their control devices are located outside the body, and transmission wires connect the actuators and body. Because this by-wire mechanism can increase the end-effector's agility, it has been adopted in several other child robots, such as Noby [39] and iCub [29]. Using pneumatic actuators is another solution to achieve high agility.

5.3 *Lifelike surface*

Different shapes and textures of the robot's surface give different visual and tactile impressions and therefore can change the way humans interact with it.

Robots that are designed mainly for visual lifelike impressions are android and animatronic robots. Repliee-R1 [12] and several animatronic babies [13] have realistic humanlike skin. Unconscious reactions, such as eye movement and brain activity, of humans when they face android robots tend to be similar to those when they face real humans [40]. This finding tells us the importance of the appearance of communication robots.

On the other hand, for realistic tactile impressions, we should design the shape of the foundation for the soft skin carefully. Bone-shaped curvilinear foundations seem to be suitable for giving realistic tactile impressions to humans. Such an exterior was made by 3D printing technology for Roboy [28], although this had no soft skin.

Robot surfaces can be used to display 'emotional' states through motions, texture changes, and so on. Generally, although few DOFs to move facial parts have been realized in the small faces of child robots, several other expressions have been realized. For example, Simbaby [35] can display a breathing chest, cyanosis (skin color turns blue), heartbeat, and so on to simulate several physiological abnormal states for medical training. Other robots such as Macra [41] (change in skin color and heart beat), Yotaro [42] (change in body temperature and runny nose), and Babyloid [11] (shed tears) also have such functions. Caregivers' responsive behaviors are regulated by little children and vice versa [43]. Thus, realistic emotional expressions of robots should be able to induce our natural responses.

Although we have to be careful about the so-called 'uncanny valley' effect [44], pursuing techniques for realizing humanlike impressions by robots should be a promising approach to advances in HRI research.

5.4 *Humanlike redundant DOFs*

Kinematic redundancy is generally given to robots to increase their flexibility and versatility [45]: Redundancy can enhance the motion performance in available postures to avoid collision with obstacles, motion smoothness by avoiding kinematic singularities, or acceleration of their end-effectors. Such enhancements would clearly also be effective for communication robots because their gestural motions can be rich in variety, smooth, and agile.

The human body has redundant DOFs and humans utilizes them effectively to communicate with others. Several child robots (e.g., Pneuborn-7II, -7III, -13 [25], CB^2 [14], Diego-san [26], iCub [29], and Roboy [28]) and adult-size robots (e.g., Kotaro [46], Kojiro [47], Kenshiro [48], and ECCEROBOT [49]) have adopted varying degrees of humanlike redundant DOFs. These robots are considered to be reasonable in design for two reasons. First, humanlike DOFs enable them to perform humanlike gestures more accurately, so we can understand their meanings intuitively, rapidly, and correctly. Experimental results have supported the idea that our recognition ability of motions is highly sensitive to human motions [50]. Second, the similar kinematic structure of robots to humans should help us in predicting their reactive postural changes to external forces, including physical contact with us, especially when these DOFs are compliant.

The understandability and predictability of robot motions are regarded as important for safe HRI [51], so humanlike DOFs seem desirable. However, we need to remember that redundant DOFs require additional space and increase the weight and control cost.

5.5 *Childlike appearance*

Most child robots have an enhanced childlike appearance in aspects other than an accurate size: a large head, large eyes, short extremities, and plump body shape. They are especially exaggerated on Babyloid [11], Muu [52], and Yotaro [42]. Such typical appearances of children, or baby schema [53], have been revealed to elicit strong positive responses and induce a motivation for caretaking in adults [54]. Several experimental results have shown that baby schema are related to cuteness perception [55–57] and that we are sensitive to baby-schema features not only in human children, but also in animal children [58] and products [59]. Even for robots, we can find them to be cute and be motivated to treat them as they are children [60]. Thus, robots with a childlike appearance are considered to be effective for HRI. However, further HRI experiments are necessary to find which features of child robots can efficiently induce a motivation for caretaking.

5.6 *Tradeoffs*

Although the characteristics above are considered to be important for HRI, existing child robots have only a few of them. Table 3 summarizes to what extent these robots realize each characteristic. Rating scores of ++, +, or - were given to each characteristic based on a survey of their published papers or available web information. For human-like DOFs, ++ means that the robot has redundant active joints in a humanlike body, + means that it has non-redundant active joints in a human-like body, and - means that it has few DOFs or non-humanlike body. For agility, we gave ++ to robots that were designed to realize higher agility than other normal humanoid robots. For mechanical softness, lifelike surface, and childlike appearance, we gave ++ if the robot had specified two features for each, such as soft joints and soft exteriors. Although this rating was based on qualitative judgments, it helped us find several tradeoffs in the design of child robots.

(1) None of the robots had the best ratings for both humanlike DOFs and a childlike figure, although there were several adult-size humanoid robots with redundant DOFs. This indicates the technical difficulty of realizing humanlike redundant DOFs in a small body.
(2) Only one robot (Keepon) had the best ratings for both agility and a lifelike surface. Probably because a lifelike surface requires dedicated additional parts, whose weight and deformation resistance make agile motions by the robot difficult.
(3) Because of the above two tradeoffs, robots with relatively high ratings in both a lifelike surface and childlike appearance tended to have lower ratings for both humanlike DOFs and agility and vice versa. The former two are mainly related to 'humans' impressions of robots, while the latter two are related to 'the robots' motion performance. Namely, there is a tradeoff between realizing of high-motion performance and lifelike impressions

Table 3. Degrees of realization of each characteristic among existing child-type robots. A score of ++, +, or - was given to each robot according to how much it satisfied the criterion as described at the bottom of the table.

Name of robots	Humanlike DOF	Agility	Mechanical softness	Lifelike surface	Childlike appearance
Affetto	++	++	++	+	++
Acroban[27]	++	+	+	-	+
Animatronic Baby[13]	+	+	+	++	++
Baby Alive[34]	-	-	++	+	++
Babybot[33]	+	+	-	-	-
Babyloid[11]	-	-	++	++	++
Diego-san[26]	++	+	+	-	+
iCub[29]	++	+	+	+	-
Infanoid[32]	+	+	-	-	+
KASPAR[5]	+	+	-	+	+
Keepon[4]	-	++	++	++	++
Macket[10]	+	+	++	+	++
Macra[41]	+	+	+	+	++
Muu[52]	-	-	++	++	++
M3-CB^2[14]	++	+	++	++	-
M3-Kindy[30]	+	+	+	-	-
M3-Neony[30]	+	++	-	-	++
Noby[39]	+	+	+	++	++
Paro[6]	-	-	++	++	++
Pneuborn-7II[25]	++	++	++	-	+
Pneuborn-13[25]	+	++	++	-	+
Repliee-R1[12]	-	-	+	++	++
Robota[3]	-	+	+	++	++
Roboy[28]	++	+	+	+	+
Simbaby[35]	-	-	++	++	++
Yotaro[42]	-	+	+	+	++
Zeno[61]	+	+	+	+	++

++ score	Rich	Violent	Soft joint + Soft exterior	in shape + in texture	Baby schema + Smallness
+ score	Standard	Calm	One of the above		
- score	Few	Almost static	None of the above		

of children.

6. Conclusion and future works

In this paper, we propose a redundant and compact upper body mechanism with mechanical softness, agility, humanlike kinematic structures, childlike appearance, and bone-shape coverings for lifelike skin. Although the current upper body does not have a lifelike skin (and thus the rating score for a lifelike surface is + for Affetto, as given in Table 3), it can serve as a platform to test several ideas for skin structures for highly human-friendly robots as well as other body structures such as the head, hands, and legs. We have done preliminary interaction experiments with Affetto, and will investigate how its body affects the interaction process with adults to obtain feedback for further improvements in its design.

On the other hand, Affetto is still not a perfect platform for HRI research. Although the mobility and control accuracy of robots are important features in HRI studies, the hardware system for Affetto is not yet appropriate for them. For example, its body is connected to a large and heavy pneumatic drive/control system, which makes it difficult to achieve precise control and several interactions such as being carried up or moving around, because of the many cables. In this regard, we were strongly inspired by the design strategies of Pneuborn-7II, -7III, and -13 [25] and CB^2 [14]. Their body components are specialized for each aim, i.e. highly-redundant and compliant DOFs in a small body and whole body mechanical softness with humanlike appearance. Although such distinctive features make motion control difficult to be effective, several control methods have been tested for them [7, 62]. Namely, they built complex but potentially effective bodies first, and then researched adequate control methods for them. Such a philosophy, in which the robots' physical embodiment is positively utilized to enhance their performance, has been advocated in several robotics fields, such as bio-inspired robotics (soft robotics) [63, 64], and cognitive developmental robotics [65]. Currently, several learning methods to estimate optimal model parameters for large DOF pneumatically actuated robots have been proposed [18, 66, 67] and they could be applicable to our robot Affetto.

Acknowledgment

This work was supported by a Grant-in-Aid for Specially Promoted Research No. 24000012 and Grant-in-Aid for JSPS Fellows No. 21 · 755.

References

[1] Fong T, Nourbakhsh I, Dautenhahn K. A survey of socially interactive robots. Robotics and Autonomous Systems. 2003;42(3-4):143–166.

[2] Goodrich MA, Schultz AC. Human Robot Interaction : A Survey. Foundations and Trends in Human-Computer Interaction. 2007;1(3):203–275.

[3] Billard A, Robins B, Nadel J, Dautenhahn K. Building robota, a mini-humanoid robot for the rehabilitation of children with autism. Assistive Technology. 2007;19.

[4] Kozima H, Michalowski MP, Nakagawa C. Keepon: A playful robot for research, therapy, and entertainment. International Journal of Social Robotics. 2008;1(1):3–18.

[5] Dautenhahn K, Nehaniv CL, Walters ML, Robins B, Kose-Bagci H, Mirza NA, Blow M. KASPAR - a minimally expressive humanoid robot for human-robot interaction research. Applied Bionics and Biomechanics. 2009;6(3-4):369–397.

[6] Shibata T, Wada K. Robot therapy: a new approach for mental healthcare of the elderly - a mini-review. Gerontology. 2011;57(4):378–86.

[7] Ikemoto S, Amor HB, Minato T, Ishiguro H, Jung B. Mutual learning and adaptation in physical human-robot interaction. IEEE Robotics & Automation Magazine. 2012;19(4):24–35.

[8] Kawai Y, Nagai Y, Asada M. Perceptual development triggered by its self-organization in cognitive learning. In: Proc. of international conference on intelligent robots and systems. 2012. p. 5159–5164.

[9] Argall BD, Billard AG. A survey of tactile human-robot interactions. Robotics and Autonomous Systems. 2010;58(10):1159–1176.

[10] Yoshikai T, Hayashi M, Kadowaki A, Goto T, Inaba M. Design and development of a humanoid with Soft 3D-deformable sensor flesh and automatic recoverable mechanical overload protection mechanism. In: Proc. of international conference on intelligent robots and systems. 2009. p. 4977–4983.

[11] Kanoh M, Shimizu T. Developing a robot Babyloid that cannot do anything. Journal of the Robotics Society of Japan (In Japanese). 2011;29(3):298–305.

[12] Ishiguro H. Android science: conscious and subconscious recognition. Connection Science. 2006; 18(4):319–332.
[13] Animatronic Baby. http://www.youtube.com/watch?v=XLLaqsXTeto. 2008.
[14] Minato T, Yoshikawa Y, Noda T, Ikemoto S, Ishiguro H, Asada M. CB2: A child robot with biomimetic body for cognitive developmental robotics. In: Proc. of the 7th ieee-ras international conference on humanoid robots. 2007. p. 557–562.
[15] Ishihara H, Yoshikawa Y, Asada M. Realistic child robot Affetto for understanding the caregiver-child attachment relationship that guides the child development. In: Proc. of {IEEE} international conference on development and learning. 2011. p. 1–5.
[16] Child physical characteristics database (in Japanese). Research Institute of Human Engineering for Quality Life. 2008. Tech Rep.
[17] Shen X, Goldfarb M. Simultaneous force and stiffness control of a pneumatic actuator. Dynamic Systems, Measurement, and Control. 2007;129:425–434.
[18] Todorov E, Hu C, Simpkins A, Movellan J. Identification and control of a pneumatic robot. In: Biomedical robotics and biomechatronics. 2010. p. 26–29.
[19] Noritsugu T, J-G P. Improvement of pneumatic robot control using disturbance observer. Journal of Robotics Society of Japan. 1994;12(4):590–595.
[20] Rao Z, Bone G. Nonlinear modeling and control of servo pneumatic actuators. IEEE Transactions on Control Systems Technology. 2008;16(3):562–569.
[21] Rahmat MF, Sunar NH, Salim SNS, Abidin MSZ, Mohd Fauzi AA, Ismail ZH. Review on modeling and controller design in pneumatic actuator control system. International Journal on Smart Sensing and Intelligent Systems. 2011;4(4):630–661.
[22] Affetto - upper body mechanism test. https://www.youtube.com/watch?v=RnYkcQaFLjE. 2013.
[23] Valdiero AC, Carlotto L. Study of the friction behavior in industrial pneumatic actuators. ABCM Symposium Series in Mechatronics. 2006;2:369–376.
[24] Tran XB, Yanada H. Dynamic friction behaviors of pneumatic cylinders. Intelligent Control and Automation. 2013;04(02):180–190.
[25] Narioka K, Niiyama R, Ishii Y, Hosoda K. Pneumatic musculoskeletal infant robots. In: Ieee/rsj international conference on intelligent robots and systems. 2009.
[26] Robot Baby Diego-San Shows Its Expressive Face on Video. http://spectrum.ieee.org/automaton/robotics/humanoids/robot-baby-diego-san. 2013.
[27] Ly O, Lapeyre M, Oudeyer PY. Bio-inspired vertebral column, compliance and semi-passive dynamics in a lightweight humanoid robot. IEEE/RSJ International Conference on Intelligent Robots and Systems. 2011;1:1465–1472.
[28] Pfeifer R, Marques H, Iida F. Soft Robotics: The Next Generation of Intelligent Machines. In: 23rd int'l conf. on artificial intelligence. 2012. p. 5–11.
[29] Tsagarakis NG, Metta G, Sandini G, Vernon D, Beira R, Becchi F, Righetti L, Santos-Victor J, Ijspeert AJ, Carrozza MC, Caldwell DG. iCub: the design and realization of an open humanoid platform for cognitive and neuroscience research. Advanced Robotics. 2007;21(10):1151–1175.
[30] Ishiguro H, Minato T, Yoshikawa Y, Asada M. Humanoid Platforms for Cognitive Developmental Robotics. Humanoid Robotics. 2011;8(3):391–418.
[31] RPC-S1. Vstone Co.,Ltd. http://www.vstone.co.jp/products/rpc_s1/index.html. 2011.
[32] Kozima H. Infanoid : an experimental tool for developmental psycho-robotics. In: International workshop on developmental study. 1999.
[33] Metta G, Panerai F, Sandini G. Babybot: a biologically inspired developing robotic agent. Proc SPIE. 2000;44:42–53.
[34] Baby Alive. Hasbro. http://www.hasbro.com/babyalive. 1992.
[35] SimBaby. Laerdal Medical. http://www.laerdal.com/jp/SimBaby. 2005.
[36] Maurer RE, Tindall JH. Effect of postural congruence on client's perception of counselor empathy. Journal of Counseling Psychology. 1983;30(2):158–163.
[37] Chartrand TL, Bargh JA. The chameleon effect: the perception-behavior link and social interaction. Personality and Social Psychology. 1999;76:893–910.
[38] Kanda T, Imai M, Ono T, Ishiguro H. Numerical analysis of body movements on human-robot interaction. Transactions of Information Processing Society of Japan (In Japanese). 2003;.
[39] Yasumoto M, Nabeshima C, Kuniyoshi Y. Acquisition of object-oriented behaviors using baby robot. In: The 28th annual conference of the rsj. 2010.
[40] Shimada M, Minato T, Itakura S, Ishiguro H. Evaluation of android using unconscious recognition.

In: The 6th ieee-ras international conference on humanoid robots. 2006. p. 157–162.

[41] Ishizaka Y, Hayashi M, Yoshikai T, Inaba M. Psycological evaluation of soft outer coverings with embedded sensing and expressing system for representation of "animacy"(In Japanese). In: The jsme conference on robotics and mechatronics. 2008.

[42] Kunimura H, Ono C, Hirai M, Matsuzaki WT, Muramoto M, Uchiyama T, Shiratori K, Hoshino J. Baby type robot YOTARO. Transactions of the Virtual Reality Society of Japan. 2010;15(3):279–288.

[43] Tronick EZ. Emotions and emotional communication in infants. The American Psychologist. 1989 Feb;44(2):112–9.

[44] Masahiro M. The Uncanny Valley. IEEE Robotics & Automation. 2012;19(2):98–100.

[45] Yoshikawa T. Analysis and control of robot manipulators with redundancy. In: Brady M, Paul R, editors. Robotics research the first international symposium. MIT Press. 1984. p. 735–747.

[46] Mizuuchi I, Yoshikai T, Sodeyama Y, Nakanishi Y, Miyadera A, Yamamoto T, Niemela T, Hayashi M, Urata J, Namiki Y, Nishino T, Inaba M. A Musculoskeletal Flexible-Spine Humanoid Kotaro Aiming at the Future in 15 Years Time. In: Proceedings of 36th international symposium on robotics (isr2005). 2005. Available from: http://cdn.intechopen.com/pdfs/48/InTech-A_musculoskeletal_flexible_spine_humanoid_kotaro_aiming_at_the_future_in_15_years_time.pdf.

[47] Mizuuchi I, Nakanishi Y, Sodeyama Y, Namiki Y, Nishino T, Muramatsu N, Urata J, Hongo K, Yoshikai T, Inaba M. An advanced musculoskeletal humanoid Kojiro. In: 7th ieee-ras international conference on humanoid robots. 2007.

[48] Nakanishi Y, Asano Y, Kozuki T, Mizoguchi H, Motegi Y, Osada M, Shirai T, Urata J, Okada K, Inaba M. Design concept of detail musculoskeletal humanoid Kenshiro" - Toward a real human body musculoskeletal simulator. In: 12th ieee-ras international conference on humanoid robots. 2012.

[49] Marques H, Jantsch M, Wittmeier S, Holland O, Alessandro C, Diamond A, Lungarella M, Knight R. ECCE1: the first of a series of anthropomimetic musculoskeletal upper torsos. In: 10th ieee-ras international conference on humanoid robots. 2010. Available from: http://ieeexplore.ieee.org/xpls/abs_all.jsp?arnumber=5686344.

[50] Johansson G. Visual perception of biological motion and a model for its analysis. Perception & Psychophysics. 1973;14(2):201–211.

[51] Heinzmann J, Zelinsky A. A safe-control paradigm for human-robot interaction. Intelligent and Robotic Systems. 1999;25(4):295–310.

[52] Okada M, Goan M. Modeling sociable artificial creatures: findings from the Muu project. In: The 13th international conference on perception and action. 2005.

[53] Lorenz K. Die angeborenen Formen moglicher Erfahrung. Zeitschrift für Tierpsychologie. 1943; 5(2):235–409.

[54] Glocker M, Langleben D. Baby schema in infant faces induces cuteness perception and motivation for caretaking in adults. Ethology. 2009;.

[55] Brooks V, Hochberg J. A psychophysical study of 'cuteness'. Perceptual and motor skills. 1960; 11(2):205.

[56] Hildebrandt Ka, Fitzgerald HE. Facial feature determinants of perceived infant attractiveness. Infant Behavior and Development. 1979;2:329–339.

[57] Lobmaier JS, Sprengelmeyer R, Wiffen B, Perrett DI. Female and male responses to cuteness, age and emotion in infant faces. Evolution and Human Behavior. 2010;31(1):16–21.

[58] Sanefuji W, Ohgami H, Hashiya K. Development of preference for baby faces across species in humans (Homo sapiens). Journal of Ethology. 2006;25(3):249–254.

[59] Miesler L, Leder H, Herrmann A. Isn't it cute : an evolutionary perspective of baby-schema effects in visual product designs. International Journal of Design. 2011;5(3):17–30.

[60] Breazeal C. Learning by Scaffolding. 1998;:1–106.

[61] Hanson D, Baurmann S, Riccio T, Margolin R, Dockins T, Tavares M, Carpenter K. Zeno: a cognitive character. In: The association for the advancement of artificial intelligence on creativity and robots. 2008.

[62] Narioka K, Hosoda K. Motor development of an pneumatic musculoskeletal infant robot. In: Ieee int'l conference on robotics and automation. 2011. p. 963.

[63] Pfeifer R. Self-organization, embodiment, and biologically inspired robotics. Science. 2007;318:1088–1093.

[64] Trivedi D, Rahn CD, Kier WM, Walker ID. Soft robotics: biological inspiration, state of the art, and future research. Applied Bionics and Biomechanics. 2008;5(3):99–117.

[65] Asada M, Hosoda K, Kuniyoshi Y, Ishiguro H, Inui T, Yoshikawa Y, Ogino M, Yoshida C. Cognitive

developmental robotics: a survey. IEEE Transactions on Autonomous Mental Development. 2009; 1(1):12–34.

[66] Hosoda K, Sekimoto S, Nishigori Y, Takamuku S, Ikemoto S. Anthropomorphic muscular-skeletal robotic upper limb for understanding embodied intelligence. Advanced Robotics. 2012;26(7):729–744.

[67] Rolf M, Steil J. Efficient exploratory learning of inverse kinematics on a bionic elephant trunk. IEEE Trans Neural Networks and Learning Systems. 2014;25(6):1147–1160.